24th INTERNATIONAL CONGRESS ON SOUND AND VIBRATION
23–27 July 2017, London

A SUBSYSTEM-BASED ANALYTICAL METHOD ON CHARACTERIZING THE VIBRO-ACOUSTICS OF HIGH-SPEED BRUSHLESS MOTORS

Lin Ji, Roberto Faventi, John Lamb, and Lukasz Kowalczyk

Dyson Technology Ltd., Malmesbury, Wiltshire, UK
email: Lin.Ji@dyson.com

Use of FEA models to assess the structural dynamics of a rotor dynamic system such as an electric motor is commonplace; this work demonstrates that the use of analytical models earlier in the design phase can be very effective to build understanding of the system even in complex cases. Missing the opportunity to use analytical models can slow down product development and limit the breadth of the design space evaluated. This work is focused on the use of analytical modeling, both in early stage development and later in the project cycle, and it demonstrates the usefulness and importance of low-fidelity models. A subsystem based analytical model was developed to simplify the vibro-acoustic prediction procedure for high-speed brushless motors. The approach is to divide the entire motor into three subassemblies; the rotor, the stator and the housing. These simplified subassemblies are individually modeled and connected via simple coupling elements. The model has been extensively validated by comparison with experimental results. Despite the inherent simplification required, the model has shown good agreement when investigating modification of motor components, and provided insight into complex coupling mechanisms. As a result, preliminary design proposals can be evaluated quickly and then passed to more expensive, higher fidelity FE tools with more certainty of a useful outcome. The model was also used to perform parametric studies evaluating the sensitivity of motor components to design changes. The validity and usefulness of analytical modeling techniques are demonstrated by modeling the dynamics of the latest high speed brush-less motor

Keywords: subsystem method, analytical modelling, brushless-motor, rotor, stator

1. Introduction

Analytical modelling is a very useful tool to reveal the inherent vibro-acoustic properties of generic, simple systems. Despite being restricted to simplified geometries and limitations on material properties and boundary conditions, analytical modelling can provide deep insights into the complicated vibro-acoustic coupling mechanisms for a range of complex built up systems. These models help to foresee/highlight the major causes of particular vibro-acoustic issues while at the same time revealing the associated key parameters/transmission paths.

In the present paper, an analytical modelling procedure is described for different assembly levels of a high-speed brushless motor used in Dyson Supersonic™ hairdryer based on the well-established subsystem methods [1-5]. Following the theoretical principle, a set of analytical models can be built up from a rigidly grounded rotor, flexibly grounded rotor, and rotor/frame/stator full

assembly, respectively. The inherent dynamic properties of different assemblies and the dynamic coupling mechanism can thus be revealed in an explicit and efficient way.

The validity, usefulness and limitations of the analytical modelling technique can be demonstrated by comparisons with the experimental results, with the influence of design changes on the vibro-acoustic response being further outlined. Similar modelling techniques can be extended to a generic range of brushless-motors.

Aided by the appropriate analytical models, sets of vibro-acoustic control measures can be derived from FE simulations and experimental tests in a much more efficient way.

2. Subsystem-based methods

Assume two subsystems (a) and (b) are connected via a stiffness spring K_c, as shown in Fig. 1.

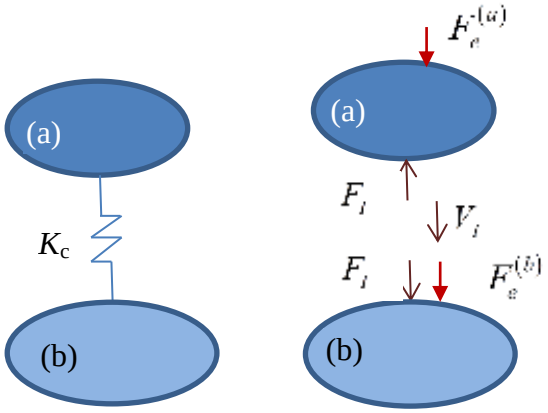

Figure 1: A generic built-up system

If subsystems (a) and (b) are subjected to external force excitations $F_e^{(a)}$ and $F_e^{(b)}$ at the locations of $x_e^{(a)}$ and $x_e^{(b)}$, respectively, the interface force F_I generated at the spring connecting locations of subsystems (a) and (b) can be expressed as

$$\frac{1}{j\omega}K_c\left(V_I^{(a)}-V_I^{(b)}\right)=F_I. \tag{1}$$

By the mobility matrix method, considering the interface force equilibrium and displacement continuity conditions, the interface velocities $V_I^{(a)}$ and $V_I^{(b)}$ can then be expressed as

$$V_I^{(a)}=Y_{eI}^{(a)}F_e^{(a)}-Y_{II}^{(a)}F_I. \tag{2}$$

$$V_I^{(b)}=Y_{eI}^{(b)}F_e^{(b)}+Y_{II}^{(b)}F_I. \tag{3}$$

where, $Y_{II}^{(a)}$ and $Y_{eI}^{(a)}$ are, respectively, the input mobility at the interface $x_I^{(a)}$ and the transfer mobility between the forcing point $x_e^{(a)}$ and the interface point $x_I^{(a)}$. Same mobility definitions are applicable for subsystem (b) in Eq. (3), with the superscript (a) being replaced by (b).

Substituting Eqs. (2) and (3) into (1), and after some algebra, gives

$$\left[Y_{II}^{(a)}+Y_{II}^{(b)}+\frac{j\omega}{K_c}\right]F_I=Y_{eI}^{(a)}F_e^{(a)}-Y_{eI}^{(b)}F_e^{(b)}. \tag{4}$$

From Eq. (4), the interface force F_I can then be obtained as

$$F_I = \left[Y_{II}^{(a)} + Y_{II}^{(b)} + \frac{j\omega}{K_c} \right]^{-1} \left[Y_{eI}^{(a)} F_e^{(a)} - Y_{eI}^{(b)} F_e^{(b)} \right]. \tag{5}$$

Substituting Eq. (5) into Eqs. (2) and (3), respectively, the interface velocities of subsystems (a) and (b), $V_I^{(a)}$ and $V_I^{(b)}$, can finally be expressed as

$$V_I^{(a)} = \left(I - Y_{II}^{(a)} \left[Y_{II}^{(a)} + Y_{II}^{(b)} + \frac{j\omega}{K_c} \right]^{-1} \right) Y_{eI}^{(a)} F_e^{(a)} + Y_{II}^{(a)} \left[Y_{II}^{(a)} + Y_{II}^{(b)} + \frac{j\omega}{K_c} \right]^{-1} Y_{eI}^{(b)} F_e^{(b)}. \tag{6}$$

$$V_I^{(b)} = \left(I - Y_{II}^{(b)} \left[Y_{II}^{(a)} + Y_{II}^{(b)} + \frac{j\omega}{K_c} \right]^{-1} \right) Y_{eI}^{(b)} F_e^{(b)} + Y_{II}^{(b)} \left[Y_{II}^{(a)} + Y_{II}^{(b)} + \frac{j\omega}{K_c} \right]^{-1} Y_{eI}^{(a)} F_e^{(a)}. \tag{7}$$

Consequently, by Eq. (5), the velocity responses at an arbitrary point of subsystems (a), $x_r^{(a)}$, or of subsystem (b), $x_r^{(b)}$ can be predicted, respectively, as

$$V_r^{(a)} = Y_{er}^{(a)} F_e^{(a)} - Y_{rI}^{(a)} \left[Y_{II}^{(a)} + Y_{II}^{(b)} + \frac{j\omega}{K_c} \right]^{-1} \left[Y_{eI}^{(a)} F_e^{(a)} - Y_{eI}^{(b)} F_e^{(b)} \right]. \tag{8}$$

$$V_r^{(b)} = Y_{er}^{(b)} F_e^{(b)} - Y_{rI}^{(b)} \left[Y_{II}^{(a)} + Y_{II}^{(b)} + \frac{j\omega}{K_c} \right]^{-1} \left[Y_{eI}^{(b)} F_e^{(b)} - Y_{eI}^{(a)} F_e^{(a)} \right]. \tag{9}$$

Clearly, for a rigid connection between subsystems (a) and (b), i.e., $K_c \to \infty$, Eqs. (5)-(9) can still be valid by putting the term $j\omega / K_c \approx 0$.

The above equations can be extended straightforwardly to multiple-point-couplings. For example, in case of two spring couplings between subsystems a and b, e.g., rotor and ground couplings via two supporting bearings, the coupling stiffness K_c can then be extended to a diagonal matrix form, as

$$\mathbf{K_c} = \begin{bmatrix} K_{c,1} & 0 \\ 0 & K_{c,2} \end{bmatrix}. \tag{10}$$

where, $K_{c,1}$ and $K_{c,2}$ represent the stiffness of each individual bearing.

Of course, the corresponding interface mobility terms $Y_{II}^{(a)}$ and $Y_{II}^{(b)}$ now both become 2×2 matrices, as $\mathbf{Y_{II}^{(a)}}$ and $\mathbf{Y_{II}^{(b)}}$, respectively. Similarly, for multiple force excitations, we can extend the transfer mobility terms $Y_{eI}^{(a)}$ and $Y_{eI}^{(b)}$ properly to be appropriate matrix forms as $\mathbf{Y_{eI}^{(a)}}$ and $\mathbf{Y_{eI}^{(b)}}$.

From the above analytical equations, the dynamic effects on the wholly assembled structure from each subsystem via $\mathbf{Y_{II}^{(a)}}$ and $\mathbf{Y_{II}^{(b)}}$, and from the interface components via $\mathbf{K_c}$ can be explicitly quantified. Therefore, such a subsystem modelling technique can be very attractive in the following two ways: (1) All the matrix terms are defined at the subsystem level, and hence it helps to avoid solving the eigen-problem for complicated, wholly coupled structures; (2) The prediction procedure allows the dynamic influences of each subsystem to be investigated separately, independently of the coupling strengths between components, and hence it is more able to reflect the local dynamic changes affecting the vibro-acoustic performance of the system as a whole.

A further advantage of the subsystem approach is the flexibility with which theoretical models can be combined with real world measurement data. In this way, a model of the assembly can be

created using purely theoretical calculations, or experimental measurements, or combinations of experimental data and theoretical models.

3. Analytical modelling of a grounded, rotor assembly

Now we may take a rigidly grounded, generic, rotor assembly, as shown in Fig. 2 as an example to demonstrate the application of the above subsystem-based analytical procedure.

3.1 Subsystem disassembly at the component interface joints

A generic brushless motor usually contains five basic components, a magnet, impeller, shaft, and two bearing supports, as shown in Fig. 2. Now, let the rotor system be disassembled down to the individual component level as shown in Fig. 3, in which, the elastic mountings between impeller/shaft and magnet shaft can also be simulated as two stiffness terms, K_{imp} and K_{mag}, as appropriate.

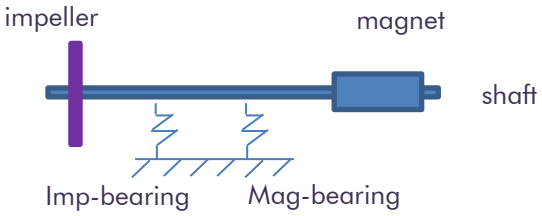

Figure 2: Rigidly grounded, brushless-rotor assembly.

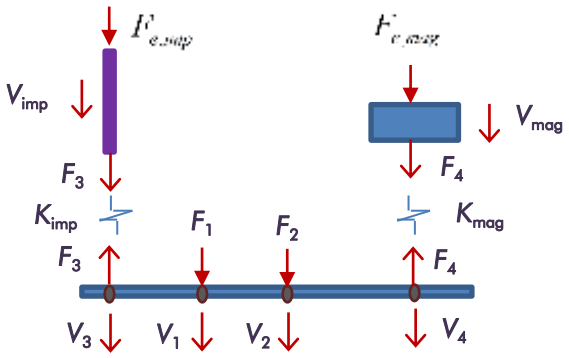

Figure 3: Exploded schematic diagram showing the velocities and forces acting at the interface joints within the rotor system.

3.2 Derive the dynamic response equations of the full rotor assembly

Following the approach outlined in Section 2, an equation of motion for each individual component can be set up. By making use of the force equilibrium and displacement continuity boundary conditions at the interface joints of any pair of directly connected components, all the interface responses can be obtained as a function of the external force excitations at each component.

For the rotor assembly of Fig. 3, the interface force acting on the shaft through the two bearing elements can be finally obtained as

$$\begin{Bmatrix} F_1 \\ F_2 \end{Bmatrix} = \left[\frac{\mathbf{K}^{(\mathrm{rotor})}}{j\omega} \right] \mathbf{A}_{12} \left(\mathbf{I} + \left[j\omega \mathbf{M}^{(\mathrm{rotor})} \right] \mathbf{A}_{22} + \left[j\omega \mathbf{M}^{(\mathrm{rotor})} \right] \left[\frac{\mathbf{K}^{(\mathrm{rotor})}}{j\omega} \right]^{-1} \right)^{-1} \begin{Bmatrix} F_{e,imp} \\ F_{e,mag} \end{Bmatrix}. \tag{11}$$

The velocity responses of the impeller and magnet can be calculated as

$$\begin{Bmatrix} V_{imp} \\ V_{mag} \end{Bmatrix} = \left[j\omega \mathbf{M}^{(\mathbf{rotor})} \right]^{-1} \begin{Bmatrix} F_{e,imp} \\ F_{e,mag} \end{Bmatrix} - \left[j\omega \mathbf{M}^{(\mathbf{rotor})} \right]^{-1} \left(\mathbf{A}_{\mathbf{22}} + \left[j\omega \mathbf{M}^{(\mathbf{rotor})} \right]^{-1} + \left[\frac{\mathbf{K}^{(\mathbf{rotor})}}{j\omega} \right]^{-1} \right)^{-1} \left[j\omega \mathbf{M}^{(\mathbf{rotor})} \right]^{-1} \begin{Bmatrix} F_{e,imp} \\ F_{e,mag} \end{Bmatrix}. \quad (12)$$

In the above equations, $\mathbf{A}_{\mathbf{11}}$, $\mathbf{A}_{\mathbf{12}}$ and $\mathbf{A}_{\mathbf{22}}$ are composed of the input- and transfer-mobility terms of the shaft, as

$$\mathbf{A}_{\mathbf{11}} = \begin{bmatrix} Y_{11}^{(shaft)} & Y_{12}^{(shaft)} \\ Y_{12}^{(shaft)} & Y_{22}^{(shaft)} \end{bmatrix}; \mathbf{A}_{\mathbf{12}} = \begin{bmatrix} Y_{13}^{(shaft)} & Y_{14}^{(shaft)} \\ Y_{23}^{(shaft)} & Y_{24}^{(shaft)} \end{bmatrix}; \mathbf{A}_{\mathbf{22}} = \begin{bmatrix} Y_{33}^{(shaft)} & Y_{34}^{(shaft)} \\ Y_{34}^{(shaft)} & Y_{44}^{(shaft)} \end{bmatrix}. \quad (13)$$

while $\mathbf{M}^{(\mathbf{rotor})}$ and $\mathbf{K}^{(\mathbf{rotor})}$ are diagonal matrices which are composed of the mass of the impeller, M_{imp}, and mass of the magnet, M_{mag}, and the mounting stiffness of impeller/shaft, K_{imp}, and that of magnet/shaft, K_{mag}, i.e.,

$$\mathbf{M}^{(\mathbf{rotor})} = \begin{bmatrix} M_{imp} & 0 \\ 0 & M_{mag} \end{bmatrix}; \quad \mathbf{K}^{(\mathbf{rotor})} = \begin{bmatrix} K_{imp} & 0 \\ 0 & K_{mag} \end{bmatrix}. \quad (14)$$

3.3 Rotor/stator full motor assembly

Fig. 3 can be further extended to include the coupling with the stator/casing subassemblies. In this case, the right-hand sides of Eqs. (11)-(12) will involve matrices which are composed of the dynamic properties of the stator and casing, as appropriate. Detailed derivations are not capitulated here for brevity. Instead, an example based on a Dyson brushless motor is given to illustrate the validity and usefulness of the above analytical procedure.

4. Theoretical application and experimental verification

The above theoretical procedure can be applied to predict either the bending motion or the axial motion of generic coupled structures, provided that the cross couplings between different types of motion can be ignored. The accuracy and validity of the above analytical procedure here is investigated by comparing the analytical predictions against the results of hammer tests in case of bending-types of vibration, in the first instance.

4.1 Analytical model

In case of the brushless motor employed in the demonstration (as shown in Fig. 4), the rotor is mounted with a rigid frame structure via the two bearing supports, and meanwhile, a stator assembly is cantilever-mounted with the frame.

If the frequency region within which each component contains no resonant modes, the stator/frame assembly can be modelled as a simple 3-DOF system, connected via two stiffness springs, as shown in Fig. 5. Here, the bonding strength between frame and bobbin and that between bobbin and stator-core components are both simulated by the effective coupling stiffness terms as K_{bob} and K_{sta}, respectively.

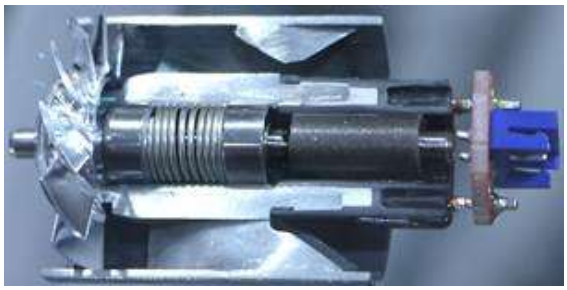

Figure 4: Main structure of the high-speed brushless motor.

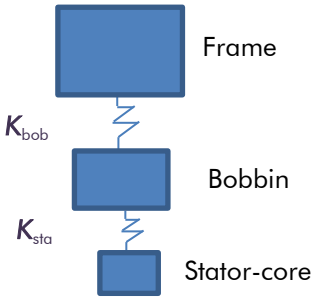

Figure 5: Illustration of frame/bobbin/stator-core assembly.

Consequently, the velocity response of the frame mass, V_{fra}, that of the bobbin mass, V_{bob}, and that of the stator-core mass, V_{sta}, can be written as

$$\{V_{fra} \quad V_{bob} \quad V_{sta}\}^T = j\omega[-\omega^2\mathbf{M}^{(\mathbf{fra/sta})} + \mathbf{K}^{(\mathbf{fra/sta})}]^{-1}\{F_{e,fra} \quad F_{e,bob} \quad F_{e,sta}\}^T. \tag{15}$$

where, $F_{e,fra}$, $F_{e,bob}$ and $F_{e,sta}$ are the external forces acting on the frame, bobbin and stator-core, respectively, while the mass matrix $\mathbf{M}^{(\mathbf{fra/sta})}$ and stiffness matric $\mathbf{K}^{(\mathbf{fra/sta})}$ can be written as

$$\mathbf{M}^{(\mathbf{fra/Sta})} = \begin{bmatrix} M_{fra} & 0 & 0 \\ 0 & M_{bob} & 0 \\ 0 & 0 & M_{sta} \end{bmatrix}; \ \mathbf{K}^{(\mathbf{fra/Sta})} = \begin{bmatrix} K_{bob} & -K_{bob} & 0 \\ -K_{bob} & K_{bob}+K_{sta} & -K_{sta} \\ 0 & -K_{sta} & K_{sta} \end{bmatrix}. \tag{16}$$

A full analytical model of the motor can then be built up by joining the subsystems in Fig. 2 and in Fig. 5 together via the two supporting bearings of the rotor/shaft.

By putting into the design parameters into the analytical modelling procedure, the low order rotor modes and the structural modes introduced by the frame/stator assembly can be predicted in an extremely efficient way. Meanwhile, major transfer function properties between any source and receiver components of the system can be revealed and highlighted.

4.2 Experimental validation

To verify the validity of the analytical model, the transfer function between the radial stator-core excitation and the impeller response were calculated and compared with the hammer test result, as shown in Fig. 6.

It is seen that the analytical prediction can capture the first few modes of both the rotor/bearing and the stator/bobbin assemblies fairly well and hence can be used to provide some insight into the

coupling mechanisms of different assemblies as well as the roles of different components within the same assembly.

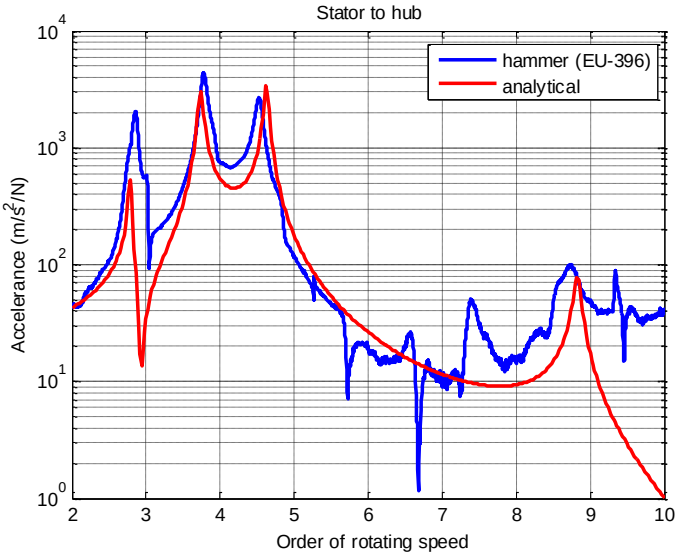

Figure 6: Comparisons of the analytical prediction and the experimental results.

5. Design application of the analytical modelling technique

Such a simple model enables the roles of different parameters which affect the inherent dynamic properties of the motor at different frequencies to be highlighted. Meanwhile, the model can reflect the vibro-acoustic influences of the major local parameter changes, and allow us to foresee the possible consequences of a design change with little computational cost. In this section, therefore, the analytical model in Section 4 is used to investigate the glue stiffness effects between the stator-core and bobbin and those between the bobbin and frame. Here, the glue stiffness effects can be modelled by varying K_{bob} and K_{sta}.

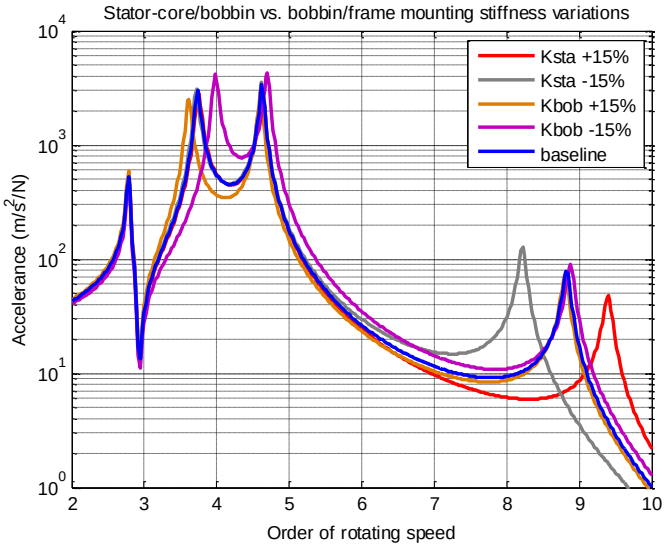

Figure 7: Comparisons of the glue stiffness effects of the stator-core/bobbin and frame/bobbin connections.

Fig. 7 compares the impeller responses when a bending force is applied to the stator-core location for different stator-core/bobbin and bobbin/frame bonding glue stiffness. It is seen that a variation of the stator-core/bobbin tends to only affect the frequency region of 8^{th}-10^{th} orders of rotating speeds, while the variations of glue strength between frame and bobbin influences the frequency

region between the 3rd-4th order of rotating speeds. One may deduce that the glue stiffness variations at the different joint locations can vary the motor acoustic performances in quite different ways.

6. Concluding remarks

In the paper, an analytical modelling technique was employed to characterize the vibro-acoustic properties of high-speed brushless motors based on subsystem analysis methods. Good agreement was observed between the analytic model and the experimental result. In principle, there are three significant advantages of analytical modelling techniques:

(1) The prediction procedure is very efficient, and the computational cost almost nil;
(2) The model is usually built up in a simple manner, but allows the major dynamics of each of the main components as well as the coupling mechanisms between them to be captured;
(3) The roles of different parameters affecting the inherent dynamic properties of the whole built-up system can be easily identified, and hence can clearly reflect the vibro-acoustic influences (at least the trends) of any major design changes.

Using analytical modelling techniques, we can foresee the possible consequences of a design change for minimal computational effort. This approach can then combine with the more accurate FE calculations and experimental results to speed up the design procedure. An analytical modelling technique is particularly useful at the concept design stages when the design details are not available for each individual component such that FE and experimental modelling techniques are not applicable.

Having said this, however, the validity of the analytical modelling technique is strongly dependent upon the simplifications which have been employed to building-up the model. The appropriate choice of model or simplification depends on the particular design purposes for that model. In general, a range of analytical models need to be employed to meet the purpose of a full vibro-acoustic analysis of any complicated structures.

Acknowledgements

The authors gratefully acknowledge their colleague David Warne for the very helpful technical discussions about this work.

REFERENCES

1 Cremer, L., Heckl, M. and Ungar, E. E., Structure-Borne Sound, 1st ed., Springer, Berlin, Heidelberg (1973).

2 Snowdon, J., Mechanical Four-pole Parameters and Their Application. Journal of Sound and Vibration, 15(3), 307-323 (1971).

3 Gardonio, P. and Brennan, M., On the Origins and Development of Mobility and Impedance Methods in Structural Dynamics". Journal of Sound and Vibration, 249(3), 557-573, 2002.

4 Gardonio, P. and Brennan, M., Mobility and Impedance Methods in Structural Dynamics: An Historical Review, Technical Report, Institute of Sound and Vibration Research (ISVR), University of Southampton (2000).

5 Ewins, D. J., Modal Testing: Theory, Practice and Application, 2nd ed., John Wiley & Sons, Inc., New York, London, Sydney (2000).

6 Craig, R. R. J. and Bampton, M. C. C., Coupling of Substructures Using Component Mode Synthesis, AIAA J. 6 (7) (1968).

7 V. van der Seijs, M., de Klerk D., and Rixen, D. J., General framework for transfer path analysis: History, theory and classification of techniques, Mechanical Systems and Signal Processing, 68-69, 217–244 (2016).